Journal of Alloys and Compounds 529 (2012) 58–62

Contents lists available at SciVerse ScienceDirect

Journal of Alloys and Compounds

journal homepage: www.elsevier.com/locate/jallcom

Extended solid solubility of a Co–Cr system by mechanical alloying

J.A. Betancourt-Cantera[a], F. Sánchez-De Jesús[a,*], G. Torres-Villaseñor[b], A.M. Bolarín-Miró[a], C.A. Cortés-Escobedo[c]

[a] Area Académica de Ciencias de la Tierra y Materiales, UAEH Carr. Pachuca-Tulancingo Km. 4.5, Pachuca, Hidalgo 42184, Mexico
[b] Instituto de Investigaciones en Materiales-UNAM, Apdo. Postal 70-360, 04510 México, DF, Mexico
[c] Centro de Investigación e Innovación Tecnológica del IPN Cda. CECATI S/N, Col. Sta. Catarina, Azcapotzalco, 02250 México, DF, Mexico

ARTICLE INFO

Article history:
Received 1 February 2012
Received in revised form 17 March 2012
Accepted 19 March 2012
Available online 28 March 2012

Keywords:
Co alloys
Co–Cr system
Phase diagram
Mechanical alloying
X-ray diffraction

ABSTRACT

Mechanical alloying, MA, has been successfully used to extend the limits of solid solubility in many commercially important metallic systems. The aim of this work is to demonstrate that MA modifies the solid solubility of the Co–Cr system. Co and Cr elemental powders were used as precursors and mixed in an adequate weight ratio to obtain $Co_{100-x}Cr_x$ ($0 \le x \le 100$, $\Delta x = 10$) to study the effect of mechanical processing in the solubility of the Co–Cr system. Processing was carried out at room temperature in a shaker mixer mill using vials and balls of hardened steel as milling media with a ball:powder weight ratio of 10:1. Crystalline structure characterization of the milled powders was conducted using X-ray diffraction, and phase transformations as a function of composition were analyzed. Thermal analysis confirmed structural changes occurred in the mechanically alloyed powders. The evolution of the phase transformations with composition is reported for each composition. The results showed that after high energy ball milling for 7 h, the solid solubility between Co and Cr could be evidently extended, despite the low solid solubility at the equilibrium conditions of this system. Additionally, the micrographs of the milled powders showed that increasing composition of chromium changes the shape and size of the particles while simultaneously reducing their agglomeration; this effect is possibly attributed to the brittleness of elemental chrome.

1. Introduction

A metallic alloy is a solid solution or homogeneous mixture of two or more metallic elements that generally has different characteristics than those of the elements that compose it; metallic alloys can be obtained by different synthesis methods. Previous studies [1] demonstrated that Mechanical Alloying (MA) is a powerful technique to synthesize nanostructured powdered materials [2–4], as long as the experimental milling conditions are well defined [5]. Recently, MA has received considerable interest because it can be used as a processing tool to obtain non-equilibrium phases [6]. It has been found that the ball milling of elemental mixtures (MA) can be employed to synthesize various metastable phases, such as supersaturated solid solutions which are immiscible [5], i.e. nanostructured materials, intermetallics [7], quasicrystalline materials and amorphous phases [8].

Phase diagrams give information about thermodynamically stable phases for a particular system (alloy) at certain pressure and temperature conditions. Alloy phase diagrams are useful to metallurgists, materials engineers and materials scientists in different areas, such as the development of new alloys for specific applications, the design and control of heat treatment procedures for specific alloys that will produce required mechanical, physical, and chemical properties, and solution of problems arising with specific alloys concerning their performance in commercial applications, thus improving product predictability [9].

Fig. 1 shows the phase diagram of the Co–Cr system studied here for the entire composition range; this diagram has been obtained by thermodynamic studies at equilibrium conditions [10]. In the Co–Cr phase diagram, there are different alloys and intermetallic compounds. An fcc phase of Co-α can be observed in the range from 0 to 40 wt% Cr, and at lower temperature, there is a peritectoid phase, an hcp phase of Co-ε, from 0 to 36 wt% Cr. At both compositions at different temperatures, total solid solutions are obtained in which the chromium is introduced in the cobalt structure, yielding two different phases. However, for a composition range from 43.9 to 100 wt% Cr at 1395 °C, there is total solubility of cobalt into the chromium structure, yielding a bcc phase of Cr-α. Within the same range from 50.5 to 63 wt% Cr at temperatures lower than 1283 °C, a congruent transformation to obtain an intermetallic CrCo-σ phase can be observed, where the solubility for both elements is partial. Additionally, in this diagram, the formation of different metastable phases can be observed.

* Corresponding author. Tel.: +527717172000x2286; fax: +527717172000x6730.
E-mail address: fsanchez@uaeh.edu.mx (F. Sánchez-De Jesús).

0925-8388/$ – see front matter © 2012 Elsevier B.V. All rights reserved.
doi:10.1016/j.jallcom.2012.03.082

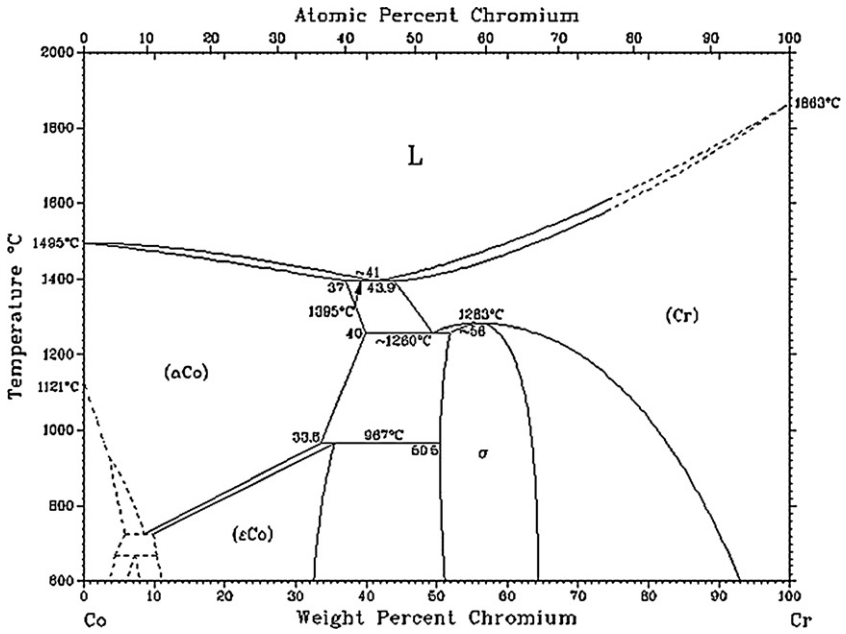

Fig. 1. Co–Cr phase diagram [9].

In this work, it is demonstrated that MA modify the solid solubility of the Co–Cr system in 7 h of milling time, when a shaker mixer/mill SPEX is used (high energy mill), in contrast with results previously reported [5,11–13] by mechanical alloying using a planetary ball mill in larger milling times.

2. Materials and methods

Co (Sigma–Aldrich, >99.9%, ℜ2 Micron) and Cr (Sigma–Aldrich, >99.9%, −325 mesh) elemental powders were used as precursors. The raw materials were mixed in the appropriated weight ratio to obtain $Co_{100-x}Cr_x$ where x varies from 0 to 100. A total amount of 5 g of the powder mixtures, as well as 6 hardened steel balls of 12.7 mm diameter, were loaded into a steel vial; the mechanical alloying process was conducted at room temperature in argon using a shaker mixer/mill machine. The ball-to-powder weight ratio was 10:1. To prevent excessive overheating of the vials, all experiments were conducted using cycles of 60 min of milling and 15 min of rest. To understand the effect of mechanical processing into the solid solubility of the Co–Cr system, compositions of $Co_{100-x}Cr_x$, with x varying from 0 to 100 and $\Delta x = 10$, were milled for 7 h.

X-ray diffraction (XRD) of the powders was used to study the phase transformations as a function of the alloy using a Bruker D8 Advance diffractometer. Diffraction parameters were 2θ ranging from 25° to 90° with a step size of 0.02(2θ). Cu Kα ($\lambda = 1.5418$ Å) radiation was used in all experiments. The stability of the synthesized powder was measured by studying the thermal behavior using a scanning differential thermal analysis (TGA/SDTA 851e Mettler–Toledo). The temperature of the structure change was estimated from a SDTA curve. The experiments were performed at a heating rate of 10 K min^{-1} using a pure argon flow of 666×10^{-3} m^3 s^{-1}.

Rietveld refinement was performed on the X-ray diffraction patterns. This method takes into account all of the information collected in a pattern, and it uses a least squares approach to refine a theoretical line profile until it matches the measured profile. This method was used to calculate the percentage of each phase for each composition. X-ray data refinement of the patterns was performed using the program MAUD [14].

Laser light diffraction was used to measure the particle size of the alloy using a Beckman Coulter LS 13320. The powder samples were dispersed in ethanol.

3. Results and discussion

According to different authors [15–22], in the Co–Cr system there is an allotropic and reversible transformation between Co (hcp) and Co (fcc) depending on the milling parameters, which is not usual at equilibrium conditions [23]. To confirm this assertion, elemental cobalt was milled for different times; X-ray diffraction patterns are shown in Fig. 2. A mixture of different crystalline structures was found: two allotropic structures of Co, Co-α (PDF # 15-0806, *Fm-3m*, fcc) and Co-ε (PDF # 05-0727, *P63/mmc*, hcp). After 1 h of milling, it is observed an increase of relative intensity of Co-hcp diffraction peaks (1 0 0) and (1 0 1) by comparing with the relative intensity of the (2 0 0) reflection peak of Co-α ($2\theta = 51.7°$). This may be related to Co allotropic transformation from fcc to hcp because Co-fcc phase is metastable at room temperature and becomes unstable when an external mechanical or thermal energy is introduced [24], on the other hand, a large number of defects are created in the fcc lattice by severe plastic deformation which cause changes to the cell parameters, giving place to hcp phase formation [25]. Therefore, when elemental Co powder is milled for 1 h, there is only one phase corresponding to the hexagonal phase of Co (hcp), which is plastically deformed in the (0 0 2) plane. After that, only a peak profile broadening can be observed by increasing milling time, as a result of a particle size refinement.

X-ray diffraction patterns for a sequence of different milled mixtures of Co and Cr elemental powders are shown in Fig. 3. In this figure, the results of milling $Co_{100-x}Cr_x$ for 7 h, with x varying from 0 to 100 and $\Delta x = 10$, are presented. As it can be observed, for $Co_{90}Cr_{10}$ and $Co_{80}Cr_{20}$ compositions, the X-ray diffraction patterns show an increase in the intensity of the Co-fcc (1 1 1) reflection and the disappearance of the Cr-bcc peaks (PDF #006-0694,

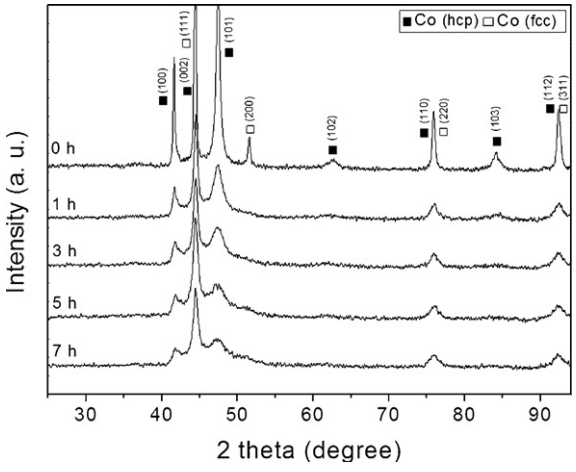

Fig. 2. XRD patterns of elemental Co powder milled for different times.

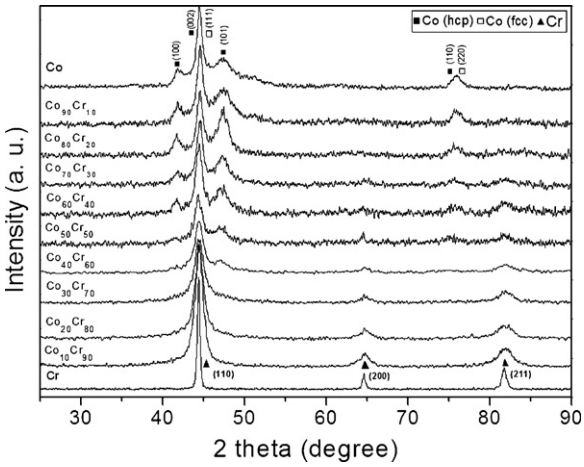

Fig. 3. XRD patterns of powder $Co_{100-x}Cr_x$ ($0 \le x \le 100$, $\Delta x = 10$) milled for 7 h.

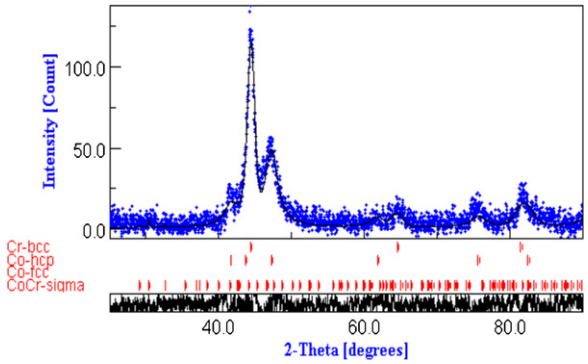

Fig. 5. Rietveld X-ray diffraction pattern refinement of $Co_{70}Cr_{30}$ mixture milled for 7 h. The difference between the experimental (dots) and the calculated (full line) patterns is given below.

Im-3m, bcc); this result can be attributed to the integration of Cr atoms into the Co-fcc structure by deformation, packing the (1 1 1) plane. In agreement with previous works [26], the Co tends to an hexagonal structure until saturation due to the deformation by MA of the cubic phase. Moreover, for compositions from $Co_{80}Cr_{20}$ to $Co_{40}Cr_{60}$ there is evidence of the development of an intermetallic compound, i.e. in Fig. 4 it is shown the X-ray pattern for powders with $Co_{70}Cr_{30}$ composition milled for 7 h. In this pattern it can be distinguished reflection peaks at 42.34°, 46.2° and 47.6° of 2θ corresponding to a sigma phase (CrCo-σ, tetragonal $P4_2/mnm$, with $a = 8.81$ Å and $c = 4.56$ Å, $c/a = 0.518$, with atomic positions reported in [27]) in small proportion (less than 5 wt%). This sigma phase has been reported to appear after annealing [5,11]. However, the formation of this phase can be attributed to the excess of energy stored in the milled powder which favors the formation of intermetallic compound. Also, at 64.85° and 81.7° of 2θ it can be seen the reflection of the planes of Cr-bcc which indicates the lack of a solid solution.

In Fig. 3 it is also observed an increase in the relative intensity of the Cr (1 1 0) plane and a diminution of the Co-hcp peak as Cr content increases (from $Co_{60}Cr_{40}$ to $Co_{40}Cr_{60}$). For these compositions, it was noted that it is not possible to obtain the total solubility of both elements because the (1 1 0), (2 0 0) and (2 1 1) planes of the Cr and the (1 0 0), (1 1 0) and (1 0 1) planes of the Co appear in the X-ray diffraction. As well as an intermetallic compound (CrCo, σ) in small proportion was formed.

Finally, in the diffraction patterns for $Co_{30}Cr_{70}$, $Co_{20}Cr_{80}$ and $Co_{10}Cr_{90}$ systems (Fig. 3) it can be observed that it is possible to obtain a total solid solution with Co and Cr for all of the compositions. The diffraction patterns show that there are no peaks from Co, and only the (1 1 0), (2 0 0) and (2 1 1) reflections corresponding to the Cr are present, confirming the introduction of the Co atoms into the Cr structure.

Rietveld refinement was performed using the XRD patterns, Fig. 5 shows the Rietveld refinement of the $Co_{70}Cr_{30}$ composition. The peaks corresponding to Co-fcc phase are not observed, only Co-hcp, Cr-bcc and CrCo-σ reflections are present. The data obtained in the Rietveld refinement for Sig and Rw are 1.305 and 33.98% respectively, those values are acceptable for materials in nanometric scale.

Fig. 6 shows some of the results of the refinements analysis, showing the percentage (wt%) of each phase for the $Co_{100-x}Cr_x$ system ($0 \le x \le 100$). Here it is observed that the Co-fcc phase is not present for any composition and the percentage of Co-hcp and intermetallic compound (σ-CoCr) decreases gradually, due to the increment of Cr-bcc. The results confirm that using MA enables total solubility for the $Co_{90}Cr_{10}$ alloy and partial solubility for the compositions from 20 to 60 Cr wt%. Finally for $x = 70$, 80 and 90 Cr wt%, it is possible to obtain a total solid solution between Co and Cr in a bcc phase. Thus, the solubility limits are modified with the MA. These data confirm the results obtained from the XRD patterns (Fig. 2).

Fig. 7 shows the SEM micrographs for the different compositions milled for 7 h. It is observed that samples with high contents of cobalt (Fig. 7a and b), present very large particle sizes caused by the ductility of cobalt, which facilitates the formation of agglomerates. However, it can be seen that increasing the chromium content causes a change in the shape and size of the particles, as well as a

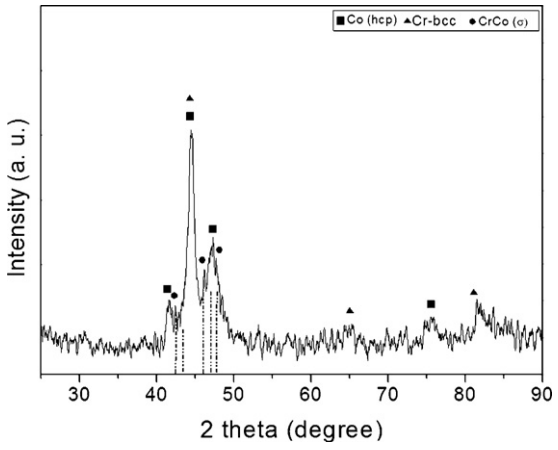

Fig. 4. XRD patterns of powder $Co_{70}Cr_{30}$ milled for 7 h.

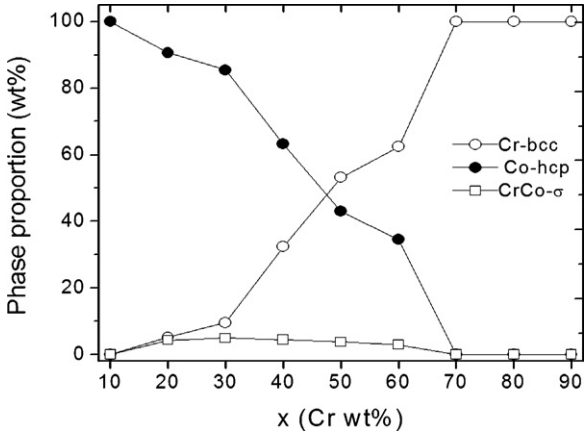

Fig. 6. Quantification of phases (wt%) and its dependence with x (Cr content) in the $Co_{100-x}Cr_x$ system milled for 7 h.

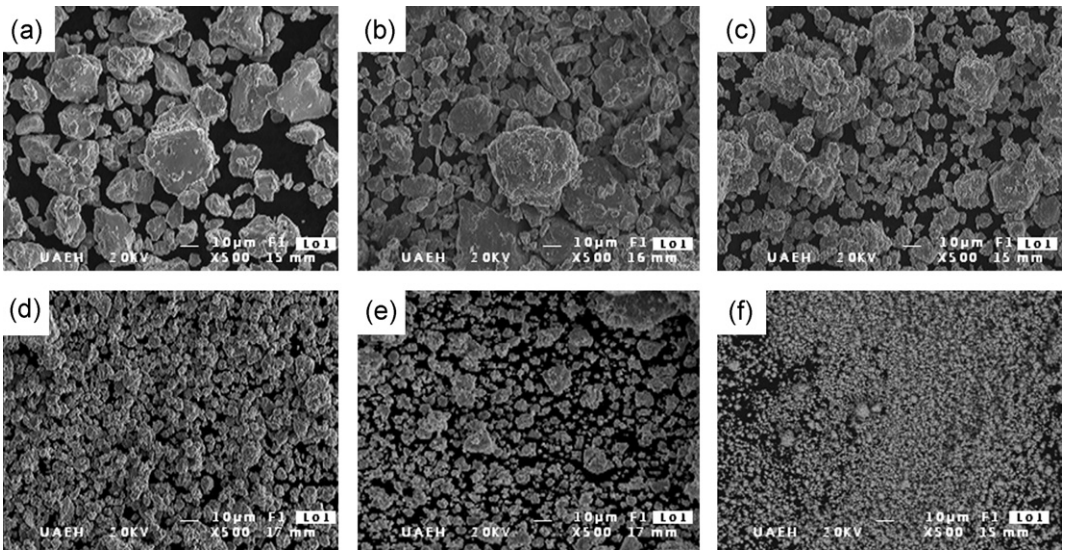

Fig. 7. SEM micrographs for different compositions milled for 7 h: (a) $Co_{90}Cr_{10}$, (b) $Co_{70}Cr_{30}$, (c) $Co_{50}Cr_{50}$, (d) $Co_{30}Cr_{70}$, (e) $Co_{20}Cr_{80}$ and (f) $Co_{10}Cr_{90}$.

decrease in the size of the agglomerates, yielding smaller particle sizes. There is also a consequent decrease in the particle size with increasing Cr content, possibly due to the brittleness of chromium. To corroborate this assertion, Fig. 8 shows the plot of cumulative volume % versus particle diameter (D) for $Co_{100-x}Cr_x$ system milled for 7 h. The results are consistent with the previously micrographs presented. It is observed a gradually dismiss of particle size with the content's chromium, from 50.12 μm to 6.65 μm for $Co_{90}Cr_{10}$ and $Co_{10}Cr_{90}$ respectively. In addition, when a solid solution of Cr-bcc has been obtained (from $Co_{30}Cr_{70}$ to $Co_{10}Cr_{90}$) it can be observed a homogeneous particle size.

Fig. 9 shows the SDTA scan for the $Co_{100-x}Cr_x$ system with x values of 10, 30, 50, 70 and 90. The SDTA results show the presence of a huge and broad exothermic peak between 750 °C and 950 °C, possibly attributed to the structural transformation of cobalt (fcc) to cobalt-hcp; this transformation occurs at different temperatures for different systems [28–30]. Besides, a consistent decrease in the transformation temperature from 914.26 °C to 835.46° C for $Co_{90}Cr_{10}$ and $Co_{10}Cr_{90}$ respectively with increasing chromium content (x) was found, possibly due to the dissolution of cobalt atoms in the structure of the chromium. Finally, it is assumed that the temperature of the thermal event (exothermic peak) can be associated to the crystallization temperature (Tc) of cobalt.

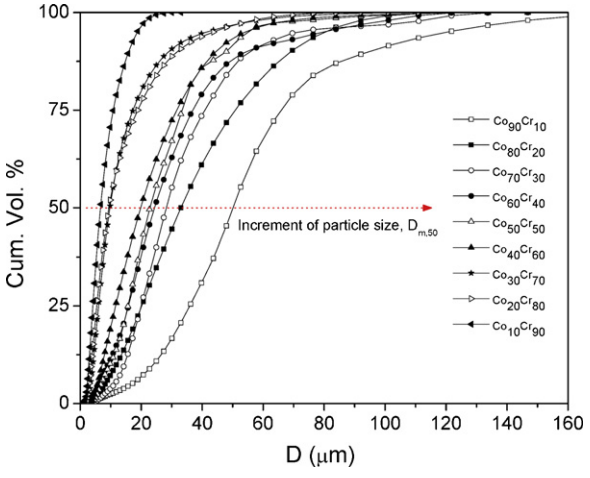

Fig. 8. Variation of the particle size of $Co_{100-x}Cr_x$ system with x from 0 to 100 and $\Delta x = 10$.

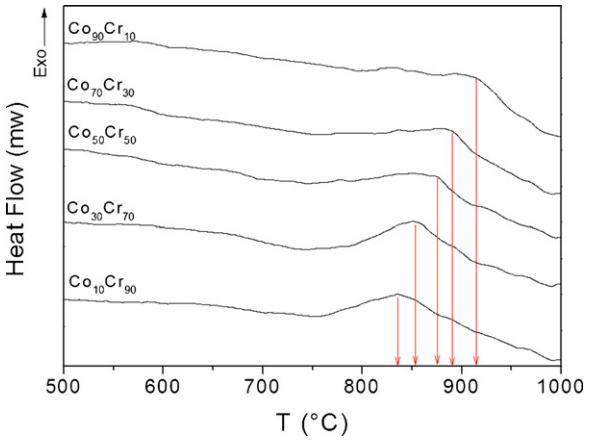

Fig. 9. SDTA curve of the $Co_{100-x}Cr_x$ system for different x value.

4. Conclusions

The results obtained showed that mechanical alloying causes an extension in the solid solubility of the $Co_{100-x}Cr_x$ system due to the mechanical energy from the milling, which forces the formation of metastable phases with greater solubility through a conversion of mechanical to surface energy. Additionally, the phase transformation of milled elemental Co from fcc to hcp structure was demonstrated after 3 h of milling. After 7 h of milling time, it is possible to produce a total solid solution for a composition of $Co_{90}Cr_{10}$ in which the solubility of the Cr atoms in the structure of the Co are complete. In addition, the Co is soluble in the chromium structure for $x = 70$, 80 and 90 wt%.

Nevertheless, a small amount of intermetallic compound with a sigma phase (CrCo) was obtained for the $Co_{100-x}Cr_x$ system from $x = 20$–60.

The results obtained from the Rietveld refinements confirm that a cobalt allotropic transformation of Co-fcc and hcp to Co-hcp exists, which disappears when $x = 70$, 80 and 90. Additionally, the CrCo-σ phase disappears, where the cobalt atoms are completely soluble in the chromium structure. An exothermic transformation occurred between 750 and 950 °C, showing possibly a structural shift due to the phase transformation to the cobalt and the increment of the chromium composition.

Acknowledgments

This project was financially assisted by the National Science and Technology Council of Mexico, CONACyT from México under grant no. 129910, 157925 and 130413. Additionally, the authors are grateful to *Maria Magdalena Marines Cruz* from DiSA, UAEH, for her many useful suggestions.

References

[1] F. Sánchez-De Jesús, A.M. Bolarín-Miró, G. Torres-Villaseñor, C.A. Cortés-Escobedo, J.A. Betancourt-Cantera, J. Mater. Sci: Mater. Med. 21-7 (2010) 2021–2026.
[2] Y.H. Zhao, K. Lu, T. Liu, J. Non-Cryst. Solids 356-43 (2010) 246–251.
[3] M.S. El-Eskandarany, Mechanical Alloying for Fabrication of Advanced Engineering Materials, Noyes Publication, New York, 2001.
[4] S. Sheibani, S. Heshmati-Manesh, A. Ataie, J. Alloys Compd. 495 (2010) 59–62.
[5] S. Louidi, F.Z. Bentayeb, W. Tebib, J.J. Suñol, A.M. Mercier, J.M. Greneche, J. Non-Cryst. Solids 356 (20–22) (2010) 1052–1056.
[6] G.J. Fan, M.X. Quan, Z.Q. Hu, J. Mater. Sci. 30 (1995) 4847–4851.
[7] J.C. Crivello, T. Nobuki, T. Kuji, Intermetallics 15 (2007) 1432–1437.
[8] S.K. Pabi, I. Manna, B.S. Murty, Bull. Mater. Sci. 22 (3) (1999) 321–327.
[9] ASM Handbook, Alloys Phase Diagrams, vol. 3, 1998, pp. 9–26, 635.
[10] C. Suryanarayana, Mechanical Alloying and Milling, Marcel Dekker, New York, 2004.
[11] J. Ecker, L. Schultz, J. Less-Common Met. 166 (1990) 293–302.
[12] S. Louidi, F.Z. Bentayeb, W. Tebib, J.J. Suñol, L. Escoda, A.M. Mercier, Mater. Chem. Phys. 132 (2012) 761–765.
[13] S. Louidi, F.Z. Bentayeb, W. Tebib, J.J. Suñol, L. Escoda, A.M. Mercier, J. Alloys Compd. (2012), doi:10.1016/j.jallcom.2011.12.083.
[14] L. Lutterotti, S. Matthies, H.R. Wenk, MAUD: a friendly Java program for material analysis using diffraction, in: IUCr Newsletter of the CPD, vol. 21, 1999, pp. 14–15.
[15] L.M. Kubalova, V.I. Fadeeva, I.A. Sviridov, Rev. Adv. Mater. Sci. 18 (2008) 360–365.
[16] S. Louidi, F.Z. Bentayeb, J.J. Suñol, L. Escoda, J. Alloys Compd. 493 (2010) 110–115.
[17] F.Z. Bentayeb, S. Alleg, J.M. Greneche, J. Alloys Compd. 434 (2007) 477–480.
[18] H. Moumeni, A. Nemamcha, S. Alleg, J.M. Greneche, Mater. Chem. Phys. 122 (2010) 439–443.
[19] J.Y. Huang, Y.K. Wu, H.Q. Ye, K. Lu, NanoStruct. Mater. 6 (5–8) (1995) 723–726.
[20] S. Alleg, F.Z. Bentayeb, R. Bensalem, C. Djebbari, L. Bessais, J.M. Greneche, Phys. Stat. Sol. A 205 (2008) 1641–1646.
[21] F. Cardellini, G. Mazzone, Philos. Mag. A 67 (6) (1992) 1289–1300.
[22] J. Sort, J. Nogués, S. Suriñach, J.S. Muñoz, M.D. Baró, Mater. Sci. Eng. A 375–377 (1–2) (2004) 869–873.
[23] M. Baricco, N. Cowlam, L. Schiffini, P.P. Macri, R. Frattni, S. Enzo, Philos. Mag. B 68 (6) (1993) 957–960.
[24] L.M. Di, H. Bakker, F.R. De Boer, Physica B 182 (1992) 91–98.
[25] S. Alleg, S. Azzaz, R. Bensalem, J.J. Suñol, S. Khene, G. Fillion, J. Alloys Compd. 482 (2009) 86–89.
[26] A.M. Bolarin-Miró, F. Sánchez-De Jesús, G. Torres-Villaseñor, C.A. Cortés-Escobedo, J.A. Betancourt-Cantera, J.I. Betancourt-Reyes, J. Non-Cryst. Solids 357 (7) (2011) 1705–1709.
[27] G.J. Dickins, A.M.B. Douglas, W.H. Taylor, Acta Cryst. 9 (1956) 297–303.
[28] J. Bonastre, L. Escoda, J. Saurina, J.J. Suñol, J.D. Santos, M.L. Sánchez, B. Hernando, J. Non-Cryst. Solids 354 (2008) 5126–5128.
[29] G.P. Vassilev, K.I. Lilova, J.C. Gachon, Intermetallics 15 (2007) 1156–1162.
[30] C.E.M. Campos, J.C. de Lima, T.A. Grandi, K.D. Machado, V. Drago, P.S. Pizani, Solid State Commun. 131 (2004) 265–270.